RESULTS FROM A QCD ANALYSIS OF THE STRUCTURE FUNCTION F_2

European Muon Collaboration

K. Moser

Fakultät für Physik

Freiburg, Germany

Abstract

The analysis of the structure function F_2 measured by the EMC in a deep inelastic muon nucleon scattering experiment is discussed in terms of perturbative QCD and higher twist contributions. The influence of mass effects and heavy quark excitation is also investigated. The averaged QCD mass scale parameter $\Lambda_{\overline{MS}}$ = 150 ± 100 MeV is in agreement with the other experiments.

1. INTRODUCTION

High precision measurements of the nucleon structure function F_2 over a wide range of x and Q^2 are available and show a clear scaling violation in deep inelastic lepton nucleon scattering. These deviations from the naive quark-parton model predictions can be explained by QCD which has the important property of asymptotic freedom; i.e. with increasing momentum transfer Q^2 of the current probe the effective coupling between quarks and gluons becomes smaller. This is expressed by the running coupling constant which in leading order is given by

$$\alpha_s(Q^2) = \frac{4\pi}{\beta_o \ln\left(\frac{Q^2}{\Lambda^2}\right)} \qquad \beta_o = \frac{33 - 2N_f}{3}$$

The mass scale parameter Λ has to be defined by the experiment.

Besides the logarithmic Q^2 dependence of F_2 predicted by QCD there are further contributions to a scale breaking with a $1/Q^2$ behaviour which may have a strong impact on tests of QCD:

- threshold effects of heavy quarks mainly at low x
- mass effects of the finite masses of the nucleons and quarks
- coherent phenomena (diquark scattering, resonance production, transverse momenta ...) expressed by the higher twist operators in the operator product expansion and more generally called higher twist contribution.

It is essential therefore to decide from the experimental data how much of the scaling violation seen is due to QCD processes and how much is due to higher twist contributions before one draws conclusions on the validity of QCD. In this contribution the use of the structure function F_2 extracted in the muon nucleon scattering experiment of the EMC[1] at CERN for testing QCD will be discussed. An interpretation of the F_2 data which have been published previously is presented. Results from a numerical evolution of the Altarelli-Parisi equations are discussed, the predictions of leading order and next-to-leading order in perturbative QCD are compared. Also a separation of higher twist effects from the leading twist part is performed.

2. THE STRUCTURE FUNCTION F_2

The present analysis is based on the measurements of the structure function $F_2(x,Q^2)$[1] in high energy muon interactions in hydrogen and iron at different beam energies. Fig. 1 shows F_2 as function of Q^2 for different x-bins as measured on the hydrogen target at beam energies of 120 and 280 GeV. Additional preliminary data for a beam energy of 200 GeV indicate a comparable Q^2-dependence. For

the determination of F_2 a value of R = 0.[2] has been chosen in agreement with the results for both targets. The data selection, the extraction of differential cross sections and the determination of the structure functions are described in detail elsewhere[1].

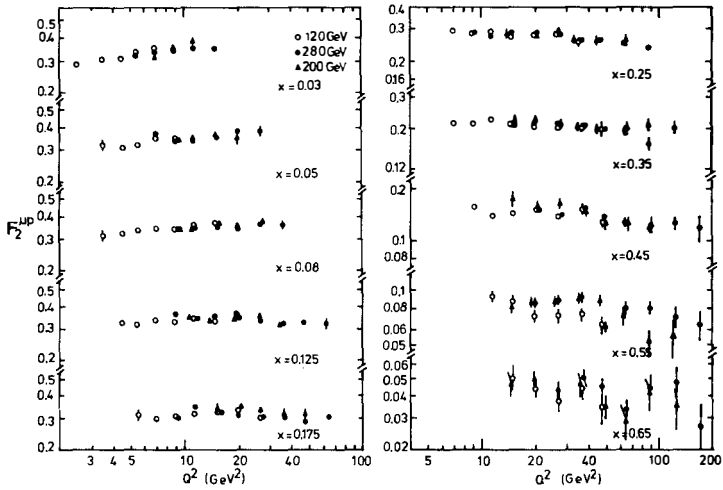

Fig. 1 The proton structure function F_2 with statistical errors as measured at different energies for R=0.

3. METHOD OF ANALYSIS

In order to test the QCD predictions and to extract the Λ parameter two equivalent methods are available: either one studies the Q^2 dependence of the moments of $F_2(x,Q^2)$ or one investigates the structure functions themselves and their Q^2 evolution as described by the Altarelli-Parisi[3] equations which express the QCD effects on quark and gluon distributions in a direct way.

The moment-method has the advantage that theoretical predictions are rather straightforward included, the Q^2 behaviour does not depend on any assumption about the x-dependence of F_2. However this approach suffers from the fact that data over the entire x range for each Q^2-bin are required. The measurements of F_2 so far are available only in a limited region of x and therefore extrapolations into regions experimentally not accessible have to be made. Higher moments are dominated by high x values where the statistics are the poorest. Successive moments are strongly correlated, the same data are used several times. At low

Q^2 contributions from elastic scattering and resonance production heavily inluence the moments.

The second method based on the Q^2 evolution of the structure functions expressed by the Altarelli-Parisi equations requires an explicit form for $F_2(x)$ at a reference point $Q^2 = Q_o^2$. The evolution equations however give the resulting F_2 at all Q^2 values so the full available data set can be used to make comparisons. The parameter Λ and the parameters governing the shape of $F_2(x,Q_o^2)$ are simultaneously adjusted until the best fit is obtained. Λ should depend neither on the chosen parametrization of $F_2(x)$ nor on the reference point Q_o^2. Moreover one has the possibility to apply suitable kinematical cuts and restrict the data analysis to regions where not well understood contributions are assumed to be negligible. Because of these advantages we favour the second technic. We use computer programs provided by Barnett et al.[4] and Gonzales - Arroyo et al.[5] to numerically integrate the Altarelli-Parisi equations in leading order and next-to-leading order.

To connect the ideas of the quark-parton model to those of QCD it is usefull to split up the structure function F_2 in a singlet and a non-singlet part. The unpaired quarks inside the nucleon, the valence quarks, contribute to flavour non-singlet distributions. Quark - antiquark pairs and the gluons coupling to them contribute to the flavour singlet structure function. Quarks radiating gluons modify both, singlet and non-singlet distributions:

$$F_2^{\mu p} = \frac{5}{18} F_2^S + \frac{3}{18} F_2^{NS}$$

$$F_2^{\mu N} = \frac{5}{18} F_2^S + \frac{3}{18} \{(c+\bar{c}) - (s+\bar{s})\}$$

and $$F_2^S = x\{(u+\bar{u}) + (d+\bar{d}) + (c+\bar{c}) + (s+\bar{s})\}$$

$$F_2^{NS} = x\{(u+\bar{u}) - (d+\bar{d}) + (c+\bar{c}) - (s+\bar{s})\}$$

4. NON-SINGLET ANALYSIS OF F_2

The distributions of the valence quarks are obviously the simplest to study. The probability distributions should show QCD distortions only due to gluon bremsstrahlung emission. Therefore we restrict our analysis in a first approach to an x-range $x \geq .25$ where valence quarks dominate keeping in mind that even for $x \geq .25$ a non negligible gluon contribution is still there and a substantial antiquark sea has been measured[6]. We solve the non-singlet Altarelli-Parisi equation:

$$\frac{dF_2^{NS}}{d \ln Q^2} = \frac{\alpha_S(Q)^2}{2\pi} \int_x^1 dz \, F_2^{NS}\left(\frac{x}{z}\right) P_{qq}(z)$$

The splitting function $P_{qq}(z)$ describes the emission of a gluon from the struck quark and is predicted by QCD. The structure function F_2^{NS} at $Q_o^2 = 4$ GeV^2 has been parametrized as

$$F_2^{NS}(x,Q_o^2) = A\, x^{\alpha}\, (1-x)^{\beta}\, (1-\gamma x)$$

and a simultaneous fit has been performed to all parameters and Λ. The results have not been significantly affected by changing Q_o^2 or the form of F_2^{NS}. Because of the invariant mass range considered four flavours have been assumed throughout the calculations. The relative normalization of the different data sets has been left free for the H_2-sample and fixed for the iron sample (3% systematics included). Extending the analysis by considering next-to-leading order corrections ($\overline{MS}$ - scheme assumed) the χ^2obtained by the fit does not differ from that one in leading order for the hydrogen data, whereas for the iron data a slightly better χ^2 than in leading order has been achieved.The calculated values for Λ are given in Table I.

Table I. Results of QCD fits to the EMC H_2 and Fe data.

Data	Λ (MeV)	χ^2/NDF
H_2	$\Lambda_{LO} = 110\ ^{+58\ +124}_{-46\ -\ 69}$	97/66
	$\Lambda_{\overline{MS}} = 139\ ^{+68}_{-56}$	99/66
Fe	$\Lambda_{LO} = 122\ ^{+22\ +114}_{-20\ -\ 70}$	211/102
	$\Lambda_{\overline{MS}} = 173\ ^{+29}_{-27}$	209/102

The results of the fits compared with the data are presented in Fig. 2 and Fig. 3. The solid lines for the large x bins are obtained by the non-singlet fits. To get an estimate how well these results describe the low x region a singlet fit in leading order was made fixing the Λ - parameter as obtained by the large x calculations (Λ_{LO} = 110 MeV for H_2 and Λ_{LO} = 122 MeV for iron) and assuming a definite form for the gluon distribution: $xG(x,Q_o^2 = 30\,\text{GeV}^2) = C\,(1-x)^5$ for the H_2 data and $xG(x,Q_o^2 = 3.5\ \text{GeV}^2) = C\,(1-x)^3$ for the iron sample. The graphic comparison of these fits with the low x bin data points is again shown in Fig. 2 and Fig. 3 indicated by the dashed lines. An explicit substraction of the sea contribution evaluated either by selecting a parametrization of Glück et al.[7] or by using the measured one from CDHS[6] has been performed. The increase of the resulting Λ of the non-singlet fit on the so corrected large x data was less than 70 MeV.

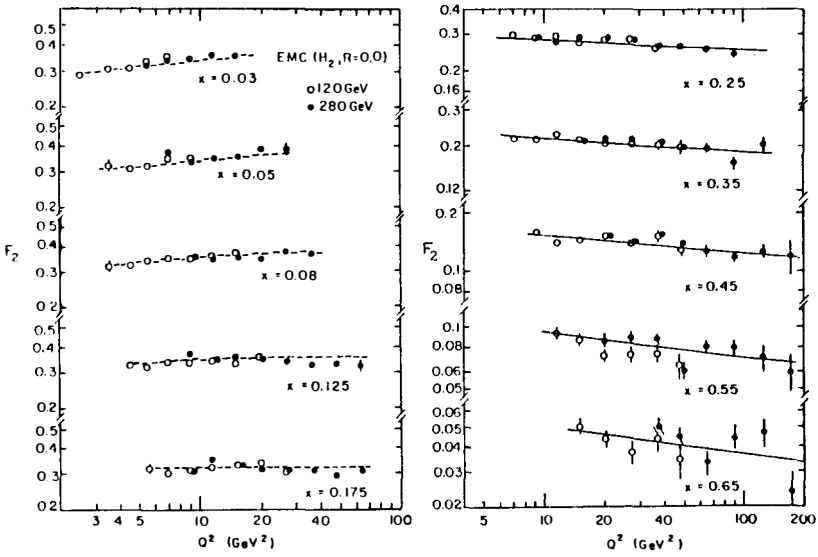

Fig. 2 $F_2^{\mu p}$ on H_2 compared with leading order QCD fits.

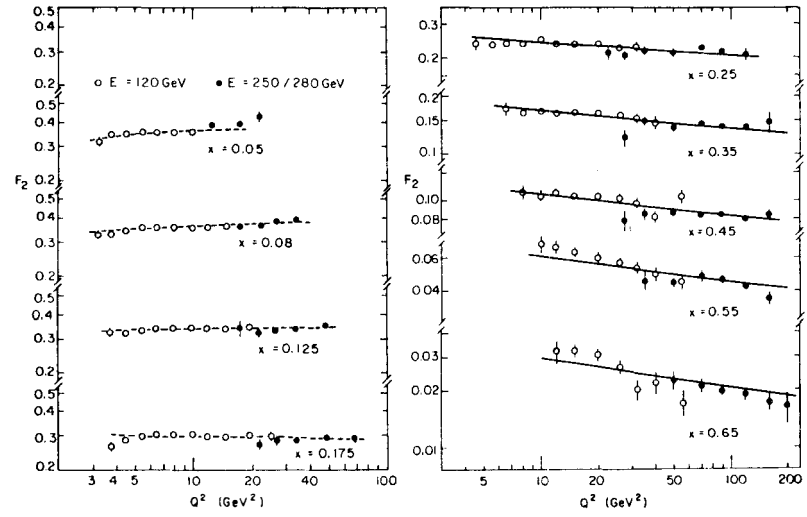

Fig. 3 $F_2^{\mu N}$ on an iron target compared with leading order QCD fits. For the details see the text.

5. SINGLET ANALYSIS OF F_2

In order to take advantage of the whole measured data set including also the low x region one has of course to treat the gluon distribution properly which is essentially concentrated and therefore most influential at low x. Moreover heavy quark production significantly influences the scaling violation and has to be taken into account. The flavour singlet evolution equations are more complicated because of additional terms and are not given here[3]. They require solving coupled integrodifferential equations, the four splitting functions are predicted by QCD but the x distributions for the gluon and the quarks have to be extracted from the data.

To investigate the possible effects of the sea contribution on Λ a parametrization of the form $xG\ (x,Q_o^2) = C\ (1-x)^n$ for the gluon has been considered leaving the power n free (C determined by the momentum sum rule). One finds a strong correlation between the power n of the gluon distribution and the value of Λ when performing a fit over the full x range (Fig. 4). A meaningfull determination of n is not possible, more sensitive calculations require additional information as input as, for instance, $F_2^{NS} = 3(F_2^p - F_2^n)$ obtained by comparison of the hydrogen with the deuterium data.

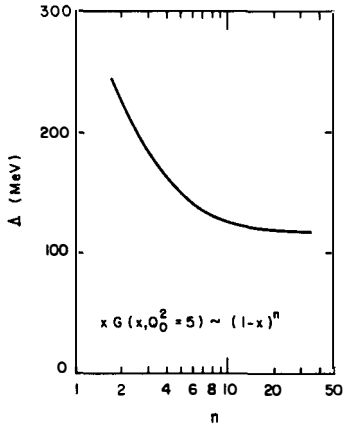

Fig. 4 Dependence of Λ on the power n of the gluon distribution for $x \geq 0.25$.

Nevertheless the increase of Λ is less than 80 MeV as long as the power n is larger than 3. A harder gluon distribution however can be excluded as recent measurements of the sea content in the nucleon show[6]. A further attempt to overcome the problems in the low x region was made by selecting an appropriate singlet structure function $F_2^S\ (x,Q_o^2) = Ax^\alpha(1-x)^\beta + B(1-x)^\gamma$ and an additional non-singlet term for the hydrogen analysis $F_2^{NS} = 3(F_2^p - F_2^n)$ parametrized by the form

$F_2^{NS}(x,Q_o^2) = C\sqrt{x}\,(1-x)^{\delta}(1-\varepsilon x)$. The parameters C, δ, ε were determined from a common fit to the SLAC[8] and the EMC deuterium data. For the gluon distribution the form $xG(x,Q_o^2) = D\,(1-x)^{5.9}\,(1+3.5x)$ according the CDHS results[6] has been chosen. To avoid effects from the charm threshold the analysis was restricted to the range $x \geq 0.08$, except for the lowest Q^2 points which were taken into account in order to constrain F_2 towards x = 0. The extracted Λ parameter (leading order only, Q_o^2 = 5 GeV^2 resp. 4 GeV^2) for the hydrogen data is

$$\Lambda^{S}_{LO} = 81\ ^{+\ 36\ +\ 44}_{-\ 30\ -\ 32}\ \text{MeV}$$

and for the isoscalar target

$$\Lambda^{S}_{LO} = 163\ ^{+\ 22\ +\ 99}_{-\ 22\ -\ 64}\ \text{MeV}$$

The Fig. 5a and 5b show the slopes $dF_2/d\ln Q^2$ from the fits for different assumptions compared with the measured points: the curves A correspond to a non-singlet fit (next to leading order), B to the singlet fit with a shape for the gluon as measured by CDHS and the curve C to a similar calculation with a rather soft gluon distribution like $\propto(1-x)^7$. In this case the Λ value obtained was 70 MeV for H_2 and 125 MeV for the iron measurements. Going to a much harder gluon distribution a la Glück et al.[7] the Λ increased to 125 MeV resp. 245 MeV. One should notice that the H_2 data favour a steeper gluon distribution.

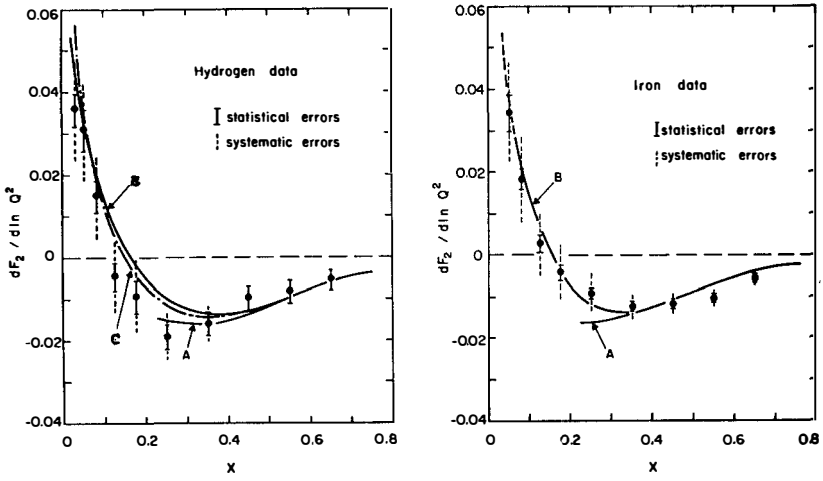

Fig. 5a,b The slopes $dF_2/d\ln Q^2$ for the H_2 and Fe data as function of x. QCD fits as described in the text.

6. THE INFLUENCE OF THE CHARM PRODUCTION

Charm threshold effects which give rise to scaling violations at very low x values have been studied systematically. In our case the QCD process governed by the photon gluon fusion graph is the most important source of heavy quark production. According the EMC results[9] on $F_2^{c\bar{c}}$ from the semileptonic decays of charmed particles a sizable contribution to the measured scaling violation of F_2 has to be accounted for (Fig. 6).

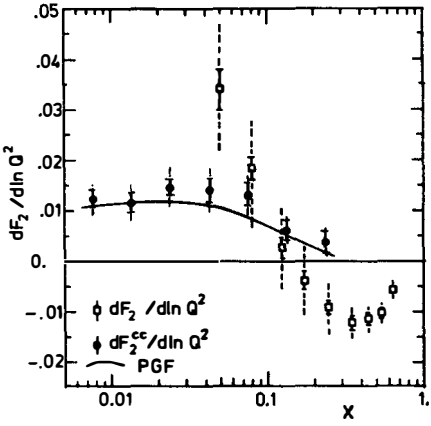

Fig. 6 The influence of charm production on the slopes of F_2. The dots correspond to the slopes of $F_2^{c\bar{c}}$ obtained from muon induced dimuon events the squares to those for $F_2^{\mu N}$. The curve indicates a typical prediction of the photon gluon fusion model.

Substracting this measured part of F_2 in a parametrized form and evaluating the fit equations assuming 3 flavours a value of Λ = 108 MeV for the hydrogen and Λ = 199 MeV for the iron data has been extracted. The results for $x \leq 0.8$ are indicated in Fig. 7 for the hydrogen case. The dashed lines correspond to the 3 flavour fit, the solid lines to the sum of the fit values for F_2 and the measured $F_2^{c\bar{c}}$ part.

7. $1/Q^2$-CONTRIBUTIONS TO THE SCALING VIOLATION

Apart from the leading twist effects which are calculable in pertubative QCD violations are also caused by contributions like target mass effects and higher twist effects[10] as mentioned earlier. Target mass corrections have been explicitely considered by replacing the x variable by ξ, the Nachtmann variable. Because of the kinematical region covered by the EMC measurements these influences are small.

It is worthwhile to investigate whether higher twist terms might account for all of the observed scaling violations or parts of it. Naively fitting the iron

F_2-data ($x \geq 0.25$) by an ansatz of $F_2(x,Q^2) = A(x) + 3.9\ x^{1.6}\ (1-x)^{1.8}/Q^2$ the measurements are well described, however performing a QCD fit and taking into account a higher twist part by adding to the leading twist term an $1/Q^2$-contribution assuming

$$F_2(x,Q^2) = F_2^{QCD}(x,Q^2) + Ax^{\alpha}\ (1-x)^{\beta}\ /Q^2$$

the χ^2 improved by 25 %. We therefore conclude that higher twist operators cannot consistently account for all the observed scaling violations. To separate a possibly existing twist 4 term a large lever arm in Q^2 is needed which can be obtained by combining low Q^2 data from SLAC[11] with the EMC measurements. The analysis was restricted to the proton-target data and to the large x region ($x \geq .25$) where a sizable higher twist contribution might be expected. Appropriate cuts to exclude resonance effects have been applied ($Q^2 \geq 1.5$ GeV^2, $W \geq 2.$ GeV). For the SLAC data their $R = 0.21$ value has been assumed. Also the relative normalization between both data sets was determined in the overlapp region independently of x. A guess function of F_2 for the non-singlet fit to leading twist 2 and twist 4 according to

$$F_2\ (x,Q^2) = F_2^{QCD}\ (1 + \frac{h_4(x)}{Q^2})$$

was chosen. Since the functional dependence of $h_4(x)$ on x is a priori unknown the fits were evaluated for each x-bin individually. The Λ parameter extracted was $\Lambda_{\overline{MS}} = 124\ ^{+\ 66}_{-\ 51}$ MeV and the resulting $h_4(x)$ values are shown in Fig. 8. The con-

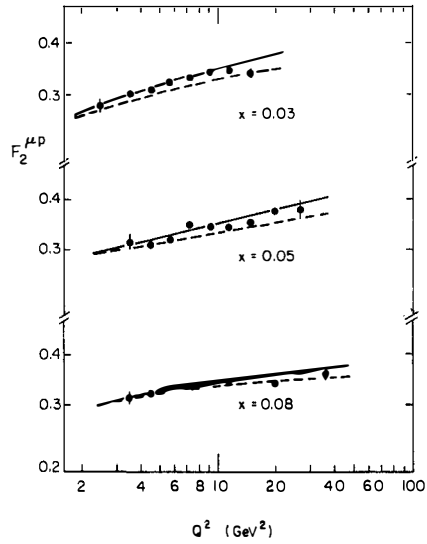

Fig. 7 F_2 of H_2 data as function of Q^2 and for $x \leq 0.08$. QCD fits as explained in the text.

sideration of a sea distribution, target mass corrections or a $R \neq 0.0$ changed indeed the Λ, but only a little the extracted $h_4(x)$ values. $h_4(x)$ is practically negligible up to $x = 0.4$ and rises steeply as function of x. An adequate description of the functional behaviour is given by a parametrization of $h_4(x) \propto x^2/(1-x)^2$ which is more likely than the usually suggested forms like $h_4(x) \propto x/(1-x)$ or $h_4(x) \propto 1/(1-x)$.

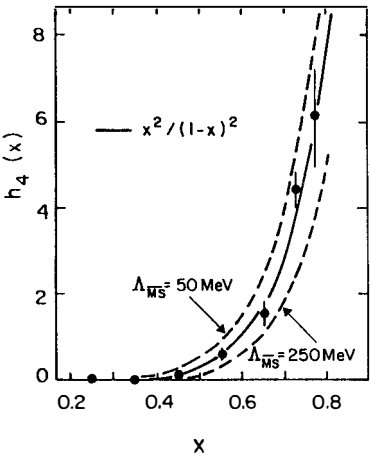

Fig. 8 $h_4(x)$, the twist 4 contribution to F_2 obtained from a fit to the SLAC-ep and EMC μp,D data using the ansatz $F_2 = F_2^{QCD}(1+h_4(x)/Q^2)$.

CONCLUSION

The observed scaling violations of F_2 seen in the muon nucleon scattering measurements of the EMC are well described by the perturbative QCD with an averaged mass scale parameter $\Lambda_{\overline{MS}} = 150 \pm 100$ MeV which corresponds to a value of $\alpha_s = 0.167 \pm \begin{matrix} 0.024 \\ 0.035 \end{matrix}$ at $Q^2 = 30\ GeV^2$ even though it is impossible to determine the gluon distribution by F_2 measurements alone. The charmed sea contributing to F_2 at low x is also well understood. At large x a consistent description of the data require an inclusion of an $1/Q^2$ higher twist term which was extracted by extending the Q^2- range by including the SLAC H_2 - data in the analysis.

REFERENCES

1. EMC, J.J. Aubert et al., Phys. Lett. 105B (1981) 315.
   Phys. Lett. 105B (1981) 322.
2. J. Drees, in Proc. of the Internatinal Symposium on Lepton and Photon Interactions at High Energies, Bonn (1981) 474.
3. G. Altarelli, G. Parisi, Nucl. Phys. B126 (1977) 298.
   G. Altarelli, in Proc. of the 14th Rencontre de Moriond (1979) 575.
4. L.F. Abbott, W.B. Atwood and R.M. Barnett, Phys. Rev. D22 (1980) 582.
5. A. Gonzales-Arroyo, C. Lopez and F.J. Yndurain, Nucl. Phys. B153 (1979) 161.
   Nucl. Phys. B159 (1979) 512.
6. CDHS, H. Abramowicz et al., CERN-EP/81-108 (1981).
7. M. Glück, E. Hoffmann and E. Reya, Report DD-TH 80/13 (1980).
8. A. Bodek et al., Phys. Rev. D20 (1979) 1471.
9. EMC, J.J.Aubert et al., CERN-EP/81-161 (1981).
10. L.F. Abbottand R.M. Barnett, Ann. Phys. 125 (1980) 276.
11. W.B. Atwood, Compilation of SLAC-DATA.